Soluble Vascular Endothelial Growth Factor Decoy Receptor FP3 Exerts Potent Antiangiogenic Effects

De-Chao Yu[1], Jung-Sun Lee[2], Ji Young Yoo[2], Hyewon Shin[2], Hongxin Deng[1], Yuquan Wei[1] and Chae-Ok Yun[3]

[1]State Key Laboratory of Biotherapy, West China Hospital, Sichuan University, Chengdu, China; [2]Brain Korea 21 Project for Medical Sciences, Institute for Cancer Research, Yonsei Cancer Center, Severance Biomedical Science Institute, Yonsei University College of Medicine, Seoul, Korea; [3]Department of Bioengineering, College of Engineering, Hanyang University, Seoul, Korea

The binding of vascular endothelial growth factor (VEGF) to its receptors stimulates tumor growth; therefore, modulation of VEGF would be a viable approach for antiangiogenic therapy. We constructed a series of soluble decoy receptors containing different VEGF receptor 1 (FLT1) and VEGF receptor 2 (KDR) extracellular domains fused with the Fc region of human immunoglobulin (Ig) and evaluated their antiangiogenic effects and antitumor effects. Results of *in vitro* binding and cell proliferation assays revealed that decoy receptor FP3 had the highest affinity to VEGF-A and -B. Compared with bevacizumab, FP3 more effectively inhibited human umbilical vein endothelial cell (HUVEC) migration and vessel sprouting from rat aortic rings. FP3 significantly reduced phosphorylation of AKT and ERK1/2, critical proteins in the VEGF-mediated survival pathway in endothelial cells. Moreover, FP3 inhibited tumor growth in human hepatocellular carcinoma (HepG2), breast cancer (MCF-7), and colorectal cancer (LoVo) tumor models, and reduced microvessel density in tumor tissues. The FP3-mediated inhibition of tumor growth was significantly higher than that of bevacizumab at the same dose. FP3 also demonstrated synergistic antitumor effects when combined with 5-fluorouracil (5-FU). Taken together, FP3 shows a high affinity for VEGF and produced antiangiogenic effects, suggesting its potential for treating angiogenesis-related diseases such as cancer.

Received 8 April 2011; accepted 30 November 2011; advance online publication 24 January 2012. doi:10.1038/mt.2011.285

INTRODUCTION

Angiogenesis is the formation of new blood capillaries from the preexisting vasculature. It plays an important role in normal embryo development, as well as repair and remodeling processes in the adult.[1] However, uncontrolled angiogenesis promotes tumor growth, metastasis, and malignancy.[2] Like many normal tissues, tumors use the vasculature to obtain oxygen and nutrients and remove waste products. Although tumors can co-opt existing host vessels, most tumors also induce new vessel formation, suggesting that neovascularization is required for their growth.[3] Consequently, much effort has been directed toward the discovery and testing of antiangiogenic agents as cancer therapeutics.

Vascular endothelial growth factor (VEFG) is a positive regulator of angiogenesis.[4,5] VEGF binds to receptors expressed on endothelial cells: VEGF receptor 1 (FLT1) and VEGF receptor 2 (KDR). FLT1 and KDR are highly related transmembrane tyrosine kinases that use their ectodomains to bind VEGF, which activates the intrinsic tyrosine kinase activity of their cytodomains and initiates intracellular signaling. The receptor-binding determinants of VEGF are localized in the N-terminal portion (amino acids 1–110), and FLT1 and KDR bind to different sites on VEGF.[6] Experiments with knockout mice deficient in either receptor revealed that FLT1 and KDR are essential for endothelial cell development.[7,8] Moreover, VEGF and its receptors are frequently upregulated in most clinically important human cancers and play a critical role in tumor-associated angiogenesis.[9]

Suppressing tumor growth and metastasis by inhibiting the activity of VEGF or its receptors exerts therapeutic effects against cancer.[3] Antiangiogenic intervention by targeting VEGF and its receptors can be accomplished through the following approaches: blocking VEGF or its receptors with neutralizing antibodies,[4,10–13] preventing VEGF from binding its cell surface receptors with soluble decoy receptors,[14,15] or targeting VEGF receptors with small molecule tyrosine kinase inhibitors.[16] Potent inhibitors of VEGF signaling such as bevacizumab (Avastin; Genentech, South San Francisco, CA), sunitinib malate (Sutent, SU11248), and sorafenib (Nexavar, BAY 43-9006) are in clinical trials or have already been approved for use in cancer. These drugs may provide a new therapeutic option for patients with bulky metastatic cancers.[17] A wide variety of antiangiogenic agents are now being tested in late-stage cancer as stand-alone agents or in combination with standard therapy.[18] The clinical promise of these initial anti-VEGF approaches highlights the need to optimize blockade of this pathway.

One of the most effective ways to block VEGF signaling is using decoy receptors to prevent VEGF from binding to its normal receptors.[3] VEGF-Trap (Aflibercept) is a soluble VEGF decoy receptor that consists of the second immunoglobulin (Ig)-like domain of FLT1 and the third Ig-like domain of KDR linked to the IgG constant region (Fc). VEGF-Trap was shown to halt angiogenesis and shrink tumors in preclinical animal models and is currently being studied in phase III clinical trials of patients with advanced solid malignancies.[19] Previous studies have demonstrated that the domain 4 of KDR is essential for receptor dimerization and enhances the association rate of VEGF to the receptor.[20,21] Studies

Correspondence: *Chae-Ok Yun, Department of Bioengineering, College of Engineering, Hanyang University, Seoul, South Korea.*
E-mail: chaeok@hanyang.ac.kr

have shown that poor pharmacokinetic properties for a fusion protein might be related to a high-positive charge of the protein.[3] Because the fourth domain of KDR has a lower isoelectric point (pI), the addition of this domain to a fusion protein decreases the positive charge of the molecule and may result in decreased adhesion to extracellular matrix.

In the present study, we generated a selective VEGF blocker (FP3) by fusing the second Ig-like domain from FLT1 and the third and the fourth Ig-like domains from KDR to human IgG1 Fc with a high-binding affinity to VEGF. FP3 effectively inhibited VEGF-induced endothelial cell proliferation, and its antiangiogenic effect was stronger than that of VEGF-Trap or bevacizumab. In addition, FP3 strongly inhibited tumor growth and significantly prolonged survival in tumor-bearing mice. The antitumor efficacy of FP3 combined with chemotherapeutic agents was greater than either single treatment. FP3 is currently in a phase I cancer trial and in a phase III study for age-related macular degeneration.

RESULTS

Generation and characterization of soluble VEGF receptor decoys

To generate a soluble decoy that binds VEGF with high affinity, a series of chimeric VEGF receptors were created by randomly fusing various extracellular domains of the VEGF receptors (FLT1 and KDR) to the Fc portion of human IgG1 (**Figure 1a**). The resulting chimeric proteins were named FP1 through FP6. Similar to VEGF-Trap, FP1 contains the extracellular domain 2 of FLT1 and extracellular domain 3 of KDR fused to the Fc portion of human IgG1. FP2 is similar to FP1, but also contains the first Ig-like domain of KDR; likewise, FP3 is similar to FP1, but also contains Ig-like domain 4 of KDR. FP4 was created by fusing the second and fourth Ig-like domains of FLT1 and the third Ig-like domain of KDR with the Fc portion of human IgG1. Similarly, FP5 has the fifth Ig-like domain of KDR in addition to the domains of FP3; FP6 has the fifth Ig-like domain of FLT1 in addition to the domains of FP4. The chimeric proteins FP2 through FP6 are designed to act as soluble decoy receptors to bind VEGF isoforms (VEGF-A, VEGF-B, and VEGF-C) and another member of the VEGF family, placenta growth factor (PlGF), thereby disrupting VEGF signaling. These fusion proteins were produced by Chinese hamster ovary cells, purified, and evaluated using the VEGF binding assay and the human umbilical vein endothelial cell (HUVEC) proliferation assay. The soluble VEGF receptor decoy FP1 (VEGF-Trap, Aflibercept[22]), was used as a control.

To test the ability of these proteins to bind and block VEGF *in vitro*, equilibrium binding assays were conducted. After different concentrations of the fusion proteins were incubated with VEGF ligands ($VEGF_{165}$, $VEGF_{121}$, VEGF-B, VEGF-C, or PlGF), the amount of unbound VEGF ligands was measured. All five chimeric proteins (FP2–FP6) bound $VEGF_{165}$ with a higher affinity than the control protein FP1 (VEGF-Trap) (**Figure 1b**). In particular, FP3 showed the highest binding activity to $VEGF_{165}$. The estimated half-maximal effective concentrations (EC_{50}) of FP1 to FP6 were 102, 46.8, 24.4, 50.2, 28.1, and 64.6 pmol/l, respectively. These fusion proteins also bound to VEGF-B, VEGF-C, and PlGF with high affinity, whereas bevacizumab bound only to VEGF-A ($VEGF_{121}$ and $VEGF_{165}$) (**Table 1**).

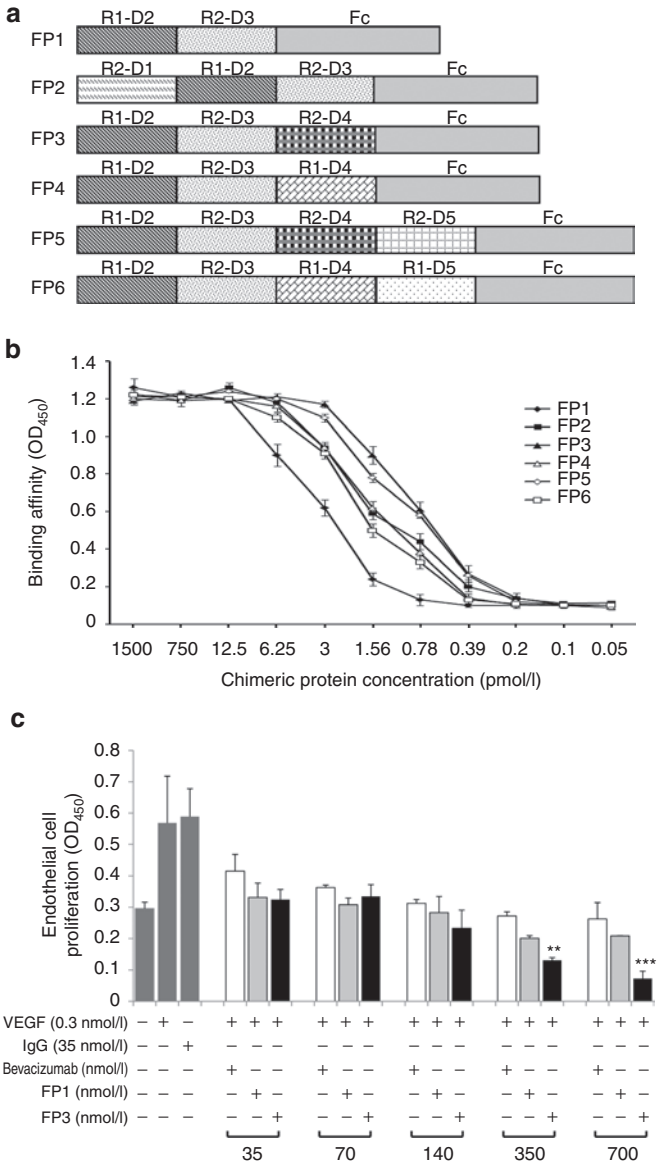

Figure 1 Schematic representation and binding affinities of chimeric decoy receptors FP1 through FP6. (**a**) The fusion proteins were constructed by fusing extracellular domains of vascular endothelial growth factor (VEGF) receptors VEGF receptor 1 (FLT1) and VEGF receptor 2 (KDR) with the Fc region of human immunoglobulin G1 (IgG1). R1 represents FLT1; R2, KDR; D1–5, Ig-like extracellular domains 1–5; Fc, human IgG1 constant region. (**b**) The binding affinities of the chimeric decoy receptors to $VEGF_{165}$ were determined. Proteins (FP1–FP6; 0.05–1,500 pmol/l) were incubated with immobilized $VEGF_{165}$ (10 pmol/l), and binding was determined by optical density at 450 nm (OD_{450}). (**c**) The inhibitory effects of chimeric proteins or bevacizumab on human umbilical vein endothelial cell (HUVEC) proliferation. Inhibition was determined by incubating the FP1, FP3, or bevacizumab (35–700 nmol/l) with $VEGF_{165}$ (0.3 nmol/l) for 3 days in endothelial basal growth medium plus 1% fetal bovine serum. Cell viability was determined using a colorimetric assay and presented as OD_{450} value. Assays were performed in triplicate and three independent experiments were conducted. $^{**}P < 0.01$, $^{***}P < 0.001$ compared with FP1.

FP3 strongly inhibits VEGF-induced angiogenesis

Since VEGF induces endothelial cell migration, proliferation, and morphogenesis, the antiangiogenic actions of the VEGF decoy receptor fusion proteins were investigated by first studying their

Table 1 Binding affinity of FP1, FP3, and bevacizumab to VEGF family members as determined by ELISA

	Binding affinity to FP1 (pmol/l)	Binding affinity to FP3 (pmol/l)	Binding affinity to bevacizumab (pmol/l)
$VEGF_{165}$	21 ± 5	6 ± 3	57 ± 12
$VEGF_{121}$	45 ± 17	26 ± 9	692 ± 214
VEGF-B	314 ± 104	122 ± 75	No binding
VEGF-C	428 ± 187	319 ± 92	No binding
PlGF	211 ± 89	147 ± 76	No binding

Abbreviations: ELISA, enzyme-linked immunosorbent assay; PlGF, placenta growth factor; VEGF, vascular endothelial growth factor.

effect on endothelial cells. As shown in **Figure 1c**, the fusion proteins (FP1 and FP3) inhibited the VEGF-induced proliferation of HUVECs by compared with cells treated with $VEGF_{165}$ alone. In addition, treatment with FP3 inhibited the VEGF-induced proliferation of endothelial cells more efficiently than either FP1 or bevacizumab, which is a VEGF-A-specific antibody widely used in clinical practice, at equimolar concentration ($P < 0.01$ at 350 and $P < 0.001$ at 700 nmol/l). These antiproliferative effects were not caused by cytotoxicity, because the fusion proteins had no effect on the normal growth of HUVECs that were not simulated with VEGF, even at doses as high as 25 µmol/l (data not shown).

The superior binding activity of FP3 to $VEGF_{165}$ and its strong inhibition of HUVEC proliferation prompted us to further explore its antiangiogenic effects. In the transwell chamber migration assay, FP3 inhibited HUVEC migration in a dose-dependent manner, with a half-maximal inhibitory concentration (IC_{50}) of 7 nmol/l (**Figure 2a**). In particular, FP3 inhibited $VEGF_{165}$-stimulated HUVEC migration more strongly than FP1 or bevacizumab at all doses tested ($P < 0.05$). (**Figure 2a**).

Angiogenesis involves multiple steps; therefore, we also evaluated the ability of FP3 to inhibit endothelial cell tube formation. On the Matrigel matrix, VEGF induces morphological differentiation of endothelial cells which sprout and fuse to form tube-like structures. In the presence of VEGF, HUVECs formed organized elongated tube-like structures resembling capillaries with an extensive network. However, cells treated with bevacizumab, FP1, or FP3 exhibited an incomplete network of capillary-like structures, inhibiting $VEGF_{165}$-induced tube formation by 34.3, 37.7, and 57.6%, respectively compared with IgG control treatment (**Figure 2b,c**). More importantly, FP3 disrupted tubule network by 31.9% and 35.5% compared with either FP1 or bevacizumab ($P < 0.01$), respectively, indicating that FP3 inhibits the tube formation step of angiogenesis more effectively than FP1 or bevacizumab.

We further tested FP3 for its ability to suppress vessel sprouting using the *ex vivo* rat aortic ring explants model. This system allows quantitative assessment of microvessel growth, maturation, and remodeling, including interactions with periendothelial cells. The number of microvessels per aortic ring was quantified at 6 days after treatment using bright field microscopy. We treated the aortic ring explants with FP3 or bevacizumab (700 and 1,400 nmol/l). Both FP3 and bevacizumab strongly inhibited microvessel growth, resulting in a marked delay in the outgrowth of sprouts from the explants, with a reduction in both length and number of vessel sprouts (**Figure 2d**). In a representative experiment (**Figure 2e**), FP3 inhibited microvessel sprouting by 70.4% and 71.2% relative to $VEGF_{165}$ treatment at 700 and 1,400 nmol/l, respectively. Compared with the same concentration of bevacizumab, FP3 treatment resulted in ~51.7% more inhibition at 700 nmol/l ($P < 0.05$) and 30% more inhibition at 1,400 nmol/l.

FP3 inhibits activation of Erk and Akt in HUVECs

To confirm that the binding interactions of FP3 to VEGF directly inhibit angiogenesis, we examined the transduction of two well characterized angiogenesis-related signals, AKT and extracellular signal-regulated kinase (ERK). VEGF activation of intracellular survival pathways in endothelial cells includes AKT and ERK; therefore, we evaluated whether FP3 is able to attenuate the activity of AKT and ERK. After pretreating HUVECs with bevacizumab, FP1, or FP3 (3 nmol/l), cells were stimulated with 10 ng/ml of $VEGF_{165}$. As shown in **Figure 3**, VEGF inhibitors bevacizumab, FP1, and FP3 inhibited VEGF-induced AKT and ERK phosphorylation. The ability of FP3 to prevent the phosphorylation of AKT and ERK appeared to be slightly better than that of bevacizumab and FP1; the ratio of pAKT/AKT for FP1 and FP3 was 0.44 and 0.15, respectively, and the ratio of pERK1/2/ERK1/2 for FP1 and FP3 was 0.82 and 0.68, respectively.

FP3 strongly suppresses tumor growth

Having shown potent antiangiogenic activity in *in vitro* and *ex vivo* models, FP3 was next evaluated in human tumor xenograft models. Two days after HepG2 human hepatocellular carcinoma cell implantation, mice were randomized into groups according to treatment: phosphate-buffered saline (PBS), 4 mg/kg FP3, 10 mg/kg FP3, 25 mg/kg FP3, or 10 mg/kg bevacizumab. The mice received treatment by intravenous (i.v.) injection twice a week for a total of seven doses. As shown in **Figure 4a**, FP3 dose-dependently reduced growth of the HepG2 tumors. Compared with the PBS-treated control group at 42 days after treatment, FP3 suppressed tumor growth by 27% at 4 mg/kg, 62% at 10 mg/kg, and 84% at 25 mg/kg. Moreover, the mean tumor volume in mice treated with 10 mg/kg FP3 (1,569 ± 239 mm^3) was smaller than that of mice treated with the same concentration of bevacizumab (2,183 ± 139 mm^3) at day 49 after treatment ($P < 0.05$).

The antitumor effects of FP3 were also evaluated in a xenograft model of human breast cancer. Animals bearing MCF-7 tumors (80–100 mm^3) were treated with FP3, bevacizumab, or PBS. As shown in **Figure 4b**, treatment with FP3 or bevacizumab significantly decreased tumor size compared with PBS ($P < 0.05$). At 35 days after treatment, FP3 suppressed tumor growth by 31.2% at 2 mg/kg, 57.4% at 6 mg/kg, and 72.7% at 18 mg/kg compared to controls; tumor growth with each incremental increase of FP3 was significantly lower than that of the previous dose.

Similarly, the antitumor efficacy of FP3 as a monotherapy was further compared to that of FP3 in a LoVo colon tumor models. The tumor volume data presented in **Figure 4c** show that treatment with FP3 resulted in significantly greater antitumor activity than treatment with FP1, showing the mean tumor volume for the tumors treated with FP1 and FP3 at 49 days after treatment was 2,022 ± 101 mm^3 and 1,020 ± 422 mm^3, respectively ($P < 0.05$).

Synergistic effects of FP3 combined with chemotherapeutic agents

To explore the therapeutic potential of FP3 in combination with chemotherapy, we assessed the antitumor effect of FP3 and 5-fluorouracil (5-FU). At day 1 after LoVo human colon carcinoma cell implantation, mice received i.v. injections of PBS, 10 mg/kg 5-FU, 6 mg/kg FP3, or FP3 combined with 5-FU; 5-FU was administered once a week, and FP3 was administered twice a week. As shown in **Figure 5a**, mean tumor volume in mice treated with PBS was higher than the mean tumor volume of all treatment groups. Compared with the PBS control on day 35 after treatment, tumor growth was inhibited by 21.1% with 5-FU alone, 45.9% with FP3 alone, and 77.8% with combination treatment of FP3 and 5-FU, demonstrating that combination therapy had the greatest effect (**$P < 0.01$ compared with 5-FU alone, *$P < 0.05$ compared with FP3 alone). **Table 2** shows the mean tumor volume of control and treatment

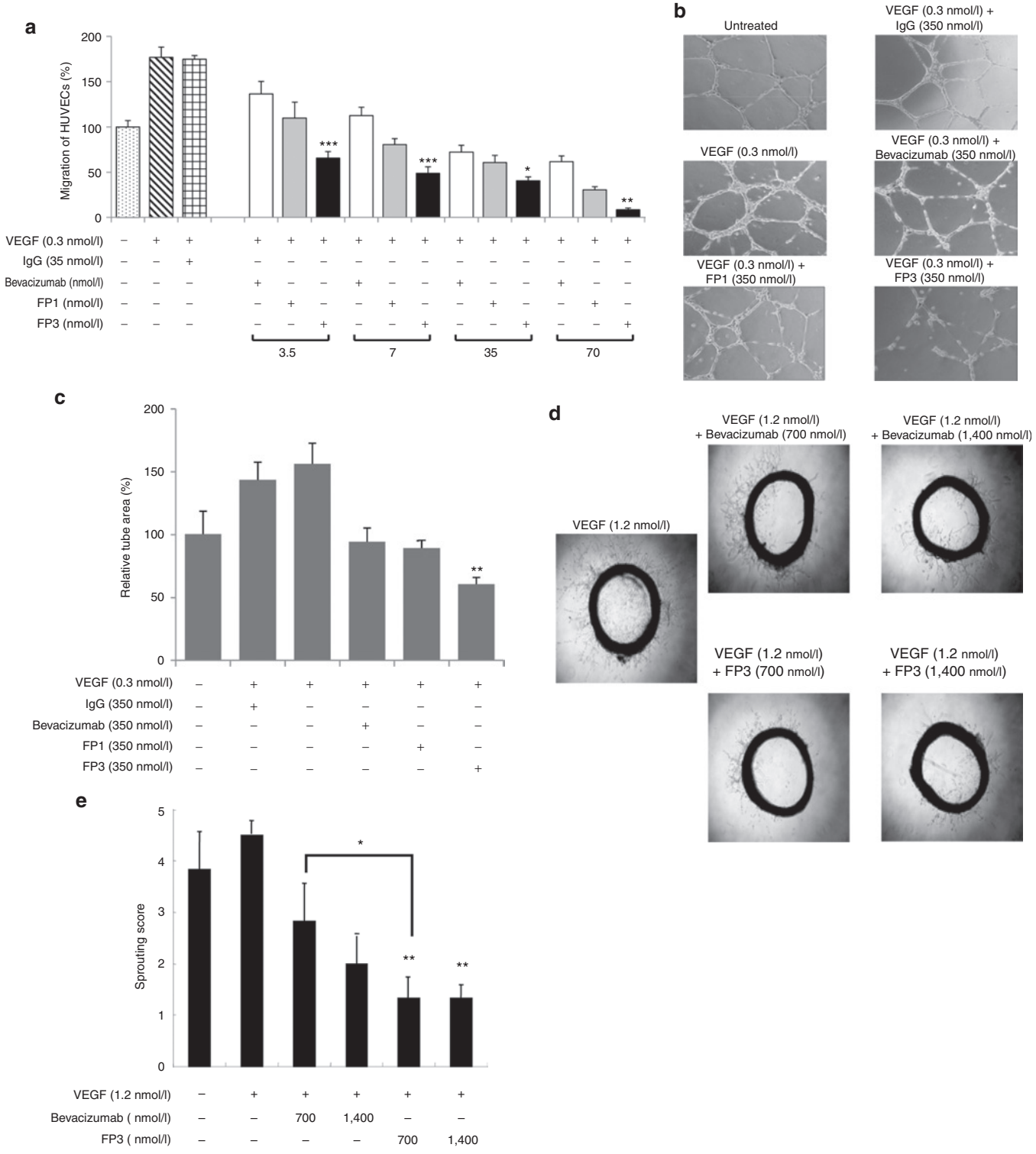

groups at four time points. Combination therapy produced a greater than additive effect (*i.e.*, synergistic effect) on tumor growth. On day 42, mice treated with combination therapy had a mean tumor volume that was 1.4-fold smaller than that expected by an additive effect. At this time point, FP3 alone inhibited tumor growth by 78% and 5-FU alone inhibited tumor growth by 50% (fractional tumor volume, 0.218 mm^3 and 0.504 mm^3, respectively) compared with the control group. These data demonstrate a synergistic effect of FP3 and 5-FU combination treatment in LoVo tumors.

Decreased angiogenesis and increased apoptosis in tumor tissues treated with combination therapy FP3 and 5-FU

Intratumoral vascularization was further assessed by CD31 immunostaining in the LoVo xenograft model. PBS-treated tumors and 5-FU-treated tumors showed abundant vasculature, which was associated with numerous pericytes (**Figure 5b**). In contrast, tumor angiogenesis was significantly suppressed by FP3 alone and FP3 plus 5-FU ($P < 0.05$), demonstrating that FP3 inhibits the proliferation and differentiation of capillary endothelial cells in tumor tissues (**Figure 5c**). Hematoxylin and eosin staining revealed necrosis in most of the remaining tumor mass after treating with FP3 alone or FP3 plus 5-FU, whereas necrotic lesions were barely detectable in tumors treated with PBS or 5-FU. As assessed by the terminal uridine deoxynucleotidyl transferase dUTP nick end labeling assay, apoptosis was markedly increased in tumors treated with FP3 alone or FP3 plus 5-FU compared with tumors treated with 5-FU (**Figure 5d**).

DISCUSSION

Aberrant angiogenesis is associated with a number of pathological conditions and diseases including cancer.[2] There is compelling evidence supporting the role of VEGF and its receptors in tumor angiogenesis, a process essential for tumor growth and metastasis.[23,24] Various approaches that disrupt or neutralize the functions of VEGF or its receptors have been tested to inhibit tumor growth and metastasis.[4,25,26] In particular, much effort has been directed toward developing antiangiogenic agents as cancer therapeutics.

In the present study, we constructed a series of soluble chimeric VEGF decoy receptors by fusing extracellular domains of FLT1 and KDR to the Fc portion of human IgG1. Among the six decoy receptors, FP3 (composed of FLT1 Ig-like domain 2 and KDR Ig-like domains 3 and 4 fused to the human IgG Fc region) showed the highest affinity to $VEGF_{165}$. Compared with FP1, FP3 also contains the KDR Ig-like domain 4, suggesting that this fourth domain may help stabilize the dimerization of the chimeric receptor protein. In addition, this fourth Ig domain contains acidic amino acids, which decrease the isoelectric point, thereby increasing the solubility of FP3 and possibly prolonging its circulation time. Shinkai *et al.* demonstrated that fourth domain of KDR is important for maintaining the high association rate of receptor-ligand association.[20] In agreement with these previous reports, we observed that FP3 had higher affinity to VEGF than FP1; EC_{50} of FP1 and FP3 is 102 and 24.4 pmol/l, respectively (**Figure 1b**). When antiangiogenic activity of FP3 was compared to that of FP1, we also observed that FP3 blocked proliferation of HUVECs more efficiently than FP1 at equimolar concentration (**Figure 1c**). Moreover, FP3 more efficiently inhibited migration and tube formation ability of HUVECs than FP1 (**Figure 2a–c**).

The best-studied and most advanced approach to blocking VEGF/KDR is the humanized monoclonal antibody bevacizumab, which is the only antiangiogenic agent approved for cancer treatment. Numerous studies have demonstrated that bevacizumab provides a survival benefit for patients with several types of cancer. In the present study, both bevacizumab and FP3 significantly suppressed VEGF-induced endothelial cell proliferation, migration, tube formation, and vessel sprouting (**Figures 1** and **2** and **Supplementary Figure S1**). Furthermore, FP3 showed a higher binding affinity to all isoforms of human VEGF and PlGF than the fusion protein FP1, which is analogous to VEGF-Trap, a decoy receptor in clinical development. This finding suggests that KDR Ig-like domain 4 may improve the antiangiogenic effects of the decoy receptor by increasing its affinity to VEGF. In marked contrast, bevacizumab did not bind to VEGF-B, VEGF-C, and PlGF (**Table 1**).

VEGF may prevent endothelial cell apoptosis through various mediators including BCL2A1, inhibitor of apoptosis, and the PI3-kinase/AKT and MAPK/ERK signal transduction pathways.[27,28] In particular, AKT and ERK play key roles in regulating cell proliferation. In the present study, the phosphorylation of AKT and ERK was significantly inhibited by FP3 in microvascular endothelial cells (**Figure 3**), suggesting that FP3 suppresses the downstream signaling of VEGF/KDR needed for endothelial cell proliferation and prevention of apoptosis.

In vivo, FP3 slowed the growth of HepG2 and MCF-7 human xenograft tumors in a dose-dependent manner and significantly delayed the time required for these tumors to reach a large size.

Figure 2 Effects of FP3 on $VEGF_{165}$-induced human umbilical vein endothelial cell (HUVEC). (**a**) Cell migration was studied using a modified transwell migration chamber. HUVECs were treated with control immunoglobulin G (IgG) (35 nmol/l) or various concentrations of bevacizumab, FP1, or FP3 in the presence of $VEGF_{165}$ (0.3 nmol/l). After 4-hour incubation at 37 °C, cells that had migrated to the lower filter surface were counted (original magnification ×200). Migration was evaluated relative to untreated cells (100%). Results are reported as the mean ± SEM of 10 independent high-power fields/well. Assays were performed in triplicate and three independent experiments were conducted. *$P < 0.05$, **$P < 0.01$, ***$P < 0.001$ compared with FP1. (**b**) The effects of bevacizumab, FP1, or FP3 on capillary tube formation (*in vitro* differentiation). HUVEC seeded on Matrigel were stimulated with $VEGF_{165}$ (0.3 nmol/l) and treated with FP1, FP3, or bevacizumab (350 nmol/l). After 20-hour incubation, cell morphology was evaluated. Representative images show organized lumen-containing structures in cells stimulated with $VEGF_{165}$ alone or human IgG plus $VEGF_{165}$ (controls) (original magnification ×100). (**c**) Area covered by the endothelial cell tube network. Results are expressed as mean ± SEM ($n = 3$). **$P < 0.01$, FP3 compared with FP1 or bevacizumab. All assays were conducted six times. (**d**) Aortic rings were embedded in Matrigel in 24-well plates and incubated for 6 days with $VEGF_{165}$ (1.2 nmol/l), and PBS, bevacizumab (700 or 1,400 nmol/l), or FP3 (700 or 1,400 nmol/l). Tissues were then fixed, stained, and photographed (original magnification ×40). (**e**) Quantitative analysis of microvessel sprouting. Microvessels were counted in high-power fields (×200), and aortic rings were assigned a rating of 0 (no sprouts) to 5 (profuse sprouting). Results are expressed as mean ± SEM. **$P < 0.01$ compared with $VEGF_{165}$; *$P < 0.05$, FP3 (700 nmol/l) compared with bevacizumab (700 nmol/l). VEGF, vascular endothelial growth factor.

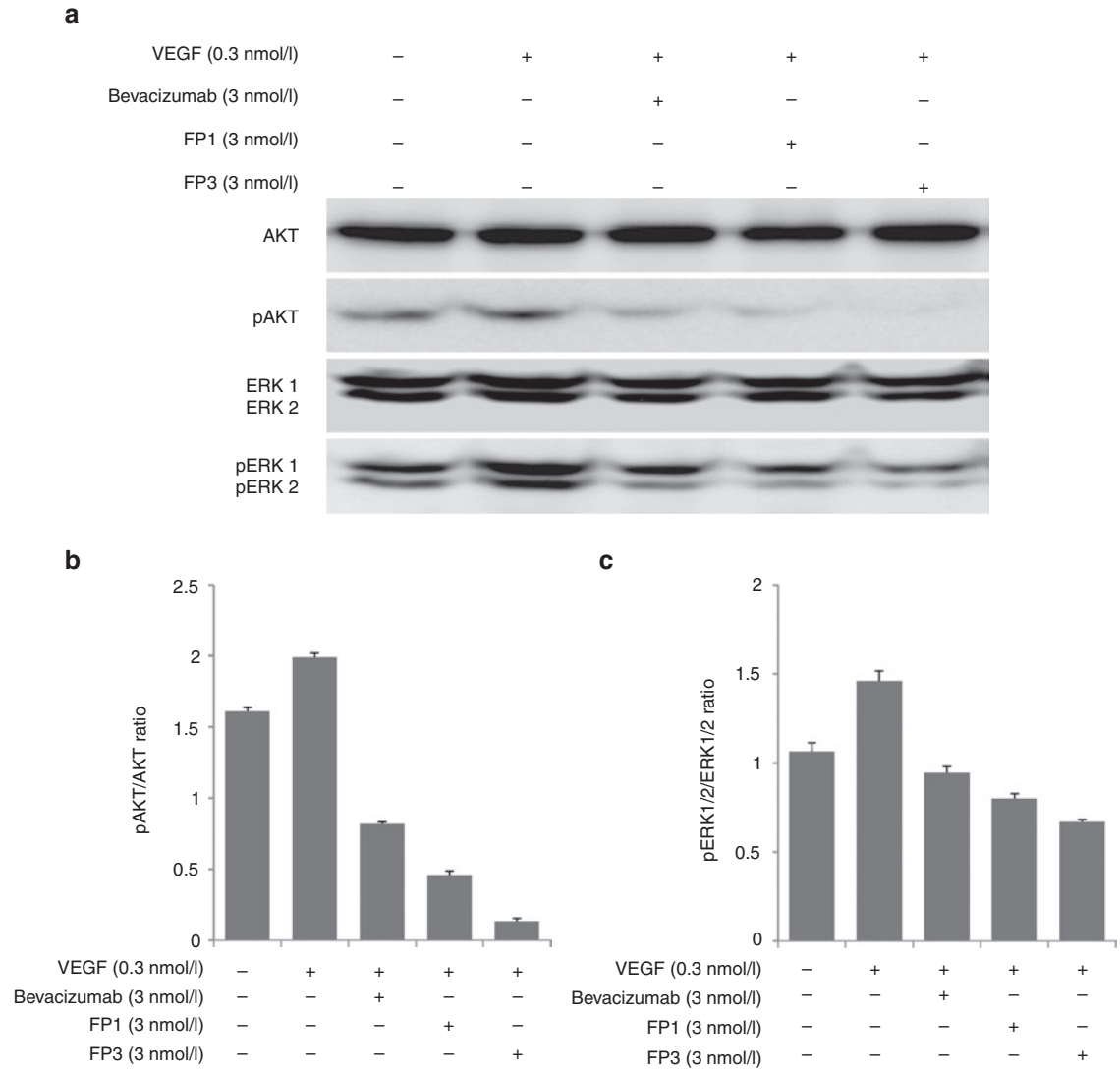

Figure 3 Effect of FP3 on ERK and AKT phosphorylation in human umbilical vein endothelial cells (HUVECs). (**a**) HUVECs were pretreated with bevacizumab, FP1, or FP3 (3 nmol/l) for 30 minutes, followed by treatment with vascular endothelial growth factor (VEGF) (10 ng/ml) for 10 minutes. Cells were harvested and analyzed by Western blot using antibodies specific to p-Akt, Akt, p-ERK1/2, or ERK1/2. β-Actin was used as a loading control. Results are representative of at least three independent experiments. (**b**) The bar graph is the ratio of phosphorylated AKT (pAKT) to total AKT. (**c**) The bar graph is the ratio of phosphorylated ERK (pERK) to total ERK.

Not only did FP3 exert a significant antitumor effect soon after tumor cell (HepG2) implantation, but FP3 also produced a marked antitumor response in established tumors (MCF-7), indicating the potential use of FP3 in the clinical setting. Moreover, FP3 showed more potent antiangiogenic effect as well as enhanced antitumor efficacy compared with FP1, demonstrating the superiority of FP3 over FP1 as therapeutic agent for cancer treatment.

Immunohistological examination of tumors from FP3-treated animals showed a decrease in microvessel density and an increase in apoptosis (**Figure 5**). The loss of microvessels in treated tumors suggests that FP3 can suppress cell survival mechanisms of the VEGF receptor-expressing tumor vasculature. This finding is consistent with previous studies that have reported that anti-VEGF treatment significantly decreases the number and size of blood vessels in tumor tissues.[29] The effects of anti-VEGF treatment may be attributed to the induction of apoptosis,[30] as well as a reduction in endothelial cell size after neutralization of endogenous VEGF. Furthermore, Skobe *et al.* reported that anti-FLK1 treatment inhibits endothelial cell proliferation in a malignant keratinocyte invasion model and induces endothelial cell apoptosis, leading to vessel regression.[26] These previous findings are consistent with the reduction in tumor vessel density in response to FP3 treatment observed in the present study, suggesting that similar mechanisms are involved.

Combining anti-VEGF agents with radiation or chemotherapeutic drugs may be a useful strategy, because radiation or chemotherapy alone is often not sufficient to completely eradicate tumors. In the present study, FP3 combined with 5-FU showed stronger antitumor actions than either treatment alone (**Figure 5**), in agreement with previous studies combining radiation[31] or chemotherapeutic drugs[32] with antiangiogenic therapy. Because VEGF functions as a survival and antiapoptotic factor in endothelial cells

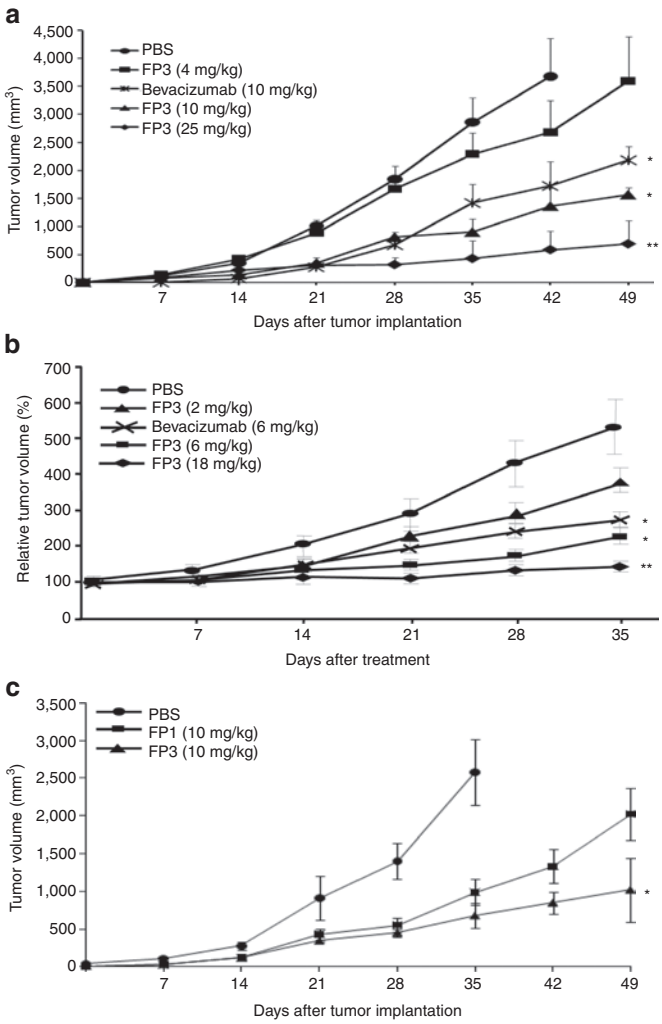

Figure 4 Effect of systemic administration of FP3 in xenograft tumor models. (**a**) Hepatocellular carcinoma HepG2 xenograft tumors after systemic administration of FP3. On day 2 following tumor cell implantation, mice were treated with phosphate-buffered saline (PBS, control), FP3 (4, 10, or 25 mg/kg), or bevacizumab (10 mg/kg) twice weekly for 7 weeks. Results are expressed as mean ± SEM. $*P < 0.05$, $**P < 0.01$ versus PBS. (**b**) Breast cancer MCF-7 xenograft tumors following systemic administration of FP3. When tumors reached the mean volume of 80–100 mm^3, mice were treated with PBS, FP3 (2, 6, or 18 mg/kg), or bevacizumab (6 mg/kg) twice weekly for 5 weeks. Tumor sizes were determined weekly. Results are expressed as mean ± SEM (each group, $n = 8$). $*P < 0.05$, $**P < 0.01$ versus PBS. (**c**). Antitumor efficacy of FP1 or FP3 in LoVo xenografts. Tumors were treated with PBS, FP1 (10 mg/kg), or FP3 (10 mg/kg) twice weekly for 7 weeks. Tumor sizes were monitored once every week. Data shown are means ± SEM (each group, $n = 8$). $*P < 0.05$ versus FP1.

in response to radiation or chemotherapy,[33,34] preventing VEGF from binding to its receptor may increase the sensitivity of tumor vasculature to chemotherapeutic agents.

FP3 is currently being tested in a phase I cancer study and a phase III clinical trial in patients with age-related macular degeneration. Preliminary data from more than 200 patients in these clinical studies demonstrate that FP3 is well-tolerated and exerts strong biological activity. In particular, the reduction of VEGF activity and formation of FP3/VEGF complexes has been reported in the circulation of cancer patients, as well as improved visual acuity for >95% of the patients with age-related macular degeneration.[35] These preliminary clinical data are consistent with results obtained from *in vitro* and *in vivo* preclinical studies, including those reported here.

In summary, we demonstrated that FP3 efficiently inhibits angiogenesis not only *in vitro* and but also *in vivo*, resulting in a potent antitumor effect. Our findings suggest that blocking the interaction between VEGF and its receptors may be a useful strategy for treating human cancer. Moreover, the use of FP3 in combination with a conventional chemotherapeutic agent produced synergistic effects. Our data show that FP3 is superior to VEGF-Trap or the humanized monoclonal antibody bevacizumab in terms of its binding affinity to VEGF and suppression of angiogenesis; therefore, FP3 may be a potential therapeutic agent for angiogenesis-related diseases such as cancers.

MATERIALS AND METHODS

Soluble chimeric VEGF receptor proteins. A series of VEGF receptor fusion proteins were generated by fusing the extracellular Ig-like domains of VEGF receptors to the Fc constant region of human IgG1 (**Figure 1a**). Using conventional polymerase chain reaction and cloning techniques, DNA fragments coding for specific domains of FLT1 and KDR were ligated in various combinations and cloned into an expression vector as described previously.[36] FP1 contains the domain 2 of VEGFR1 (from amino acids #129 to # 223) and the domain 3 of VEGFR2 (from amino acid # 225 to # 327) fused to the Fc portion of human IgG1. FP3 contains the domain 2 of VEGFR1 (from amino acids #129 to #223), the domain 3 of VEGFR2 (from amino acid #225 to #327), and the domain 4 of VEGFR2 (from amino acid # 327 to # 403) fused to the Fc portion of human IgG1. All chimeric proteins were produced in Chinese hamster ovary cells and purified using conventional methods.

Cell culture. Breast cancer (MCF-7), hepatoma (HepG2), and colon cancer (LoVo) cell lines purchased from the American Type Culture Collection (Manassas, VA) were cultured in Dulbecco's modified Eagle's medium (Gibco BRL, Grand Island, NY) supplemented with 10% fetal bovine serum (FBS; Gibco BRL), L-glutamine (2 mmol/l), penicillin (100 IU/ml), and streptomycin (50 µg/ml). HUVECs isolated from human umbilical cord veins were purchased from Clonetics (San Diego, CA) and maintained in M199 medium (Invitrogen, Carlsbad, CA) containing 20% FBS, penicillin–streptomycin (100 IU/ml), 3 ng/ml basic fibroblast growth factor (Upstate Biotechnology, Lake Placid, NY), and 5 U/ml heparin. HUVECs were used for experiments in passages 2 through 7. All cell lines were maintained at 37 °C in a humidified atmosphere at 5% CO_2.

VEGF binding assay. Affinities of the chimeric proteins to VEGF were determined by enzyme-linked immunosorbent assay (ELISA) (R&D Systems, Minneapolis, MN). The chimeric proteins (0.05–1,500 pmol/l) were incubated with immobilized VEGF isoforms/members (10 pmol/l) $VEGF_{165}$, $VEGF_{121}$, VEGF-B, VEGF-C, and PlGF (R&D Systems). After washing, the bound chimeric proteins were detected by blocking with horseradish peroxidase-conjugated goat anti-human IgG Fc (Bethyl Laboratories, Montgomery, TX). After color development, optical density at 450 nm (OD_{450}) was determined with an ELISA plate reader (Molecular Devices, Sunnyvale, CA) as described previously.[36]

HUVECs proliferation assay. To measure endothelial cell proliferation, HUVECs were seeded in gelatin-coated 48-well plates (4×10^4 cells/well). After 24 hours, cells were washed twice with endothelial basal growth medium (EBM; Clonetics) and incubated for 6 hours in EBM containing 1% FBS. Cells were incubated with different concentrations of bevacizumab, FP1, or FP3 in the presence of 0.3 nmol/l $VEGF_{165}$ (Upstate

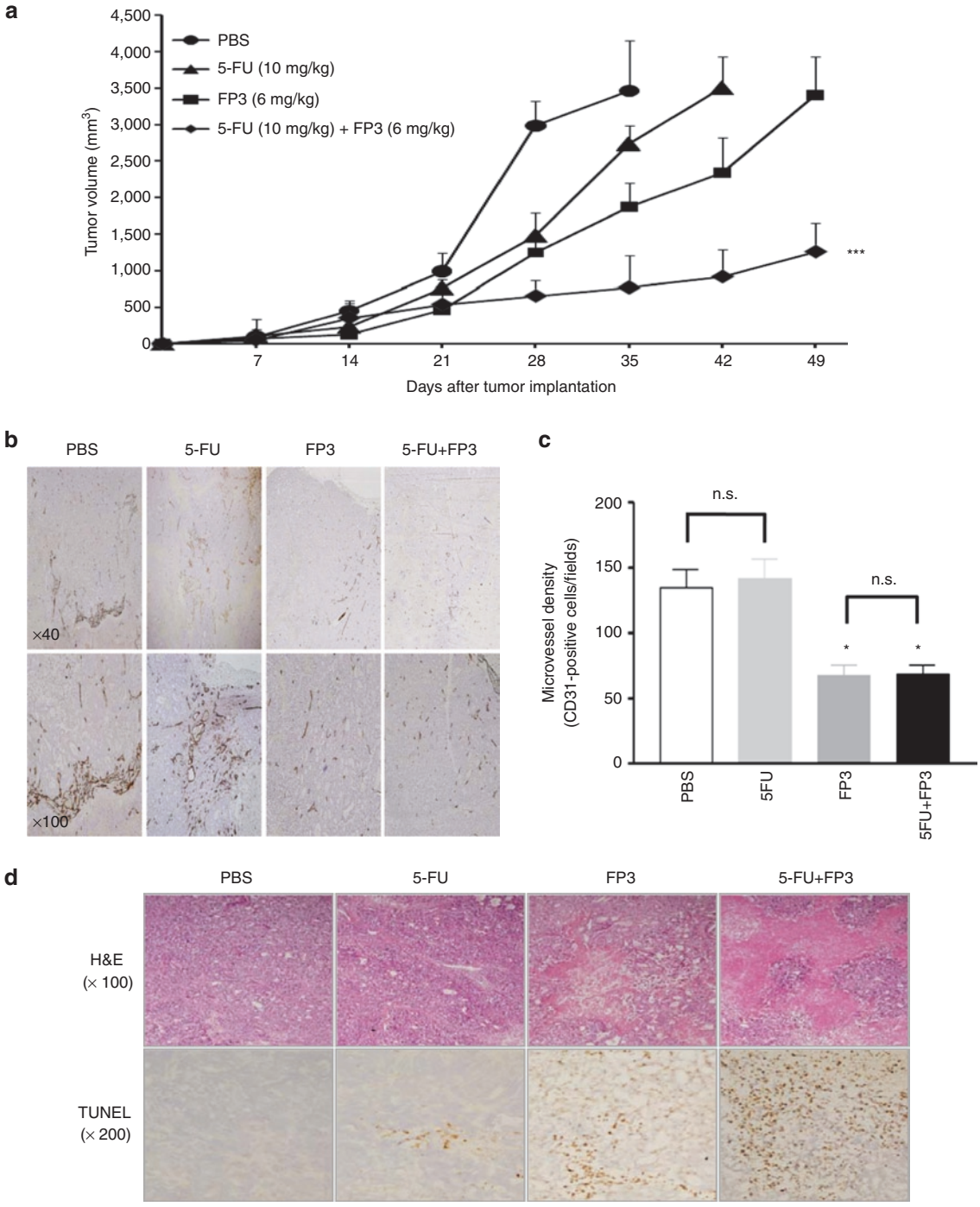

Figure 5 Effect of FP3 combined with 5-fluorouracil (5-FU) in colorectal cancer LoVo xenograft tumor model. (**a**) Mice were randomized to receive PBS, FP3, 5-FU, FP3 combined with 5-FU. FP3 (6 mg/kg) was administered twice weekly and 5-FU (10 mg/kg) once per week by intravenous injection for 7 weeks. Results are expressed as mean ± SEM. *$P < 0.05$ compared with FP3 alone, **$P < 0.01$ compared with 5-FU alone. (**b**) Immunohistochemical analysis. Intratumoral vascularization was assessed by CD31 immunostaining 5 weeks after treatment. Tissues were counterstained with H&E (original magnification ×40, ×100). (**c**) Microvessel density. Mean microvessel density was determined as $CD31^+$ cells/field. Results are expressed as mean ± SEM ($n = 3$). *$P < 0.05$ versus PBS or 5-FU; n.s., not significant. (**d**) Representative tumor sections. Tumors were stained with H&E (original magnification ×100), and apoptosis was evaluated by terminal uridine deoxynucleotidyl transferase dUTP nick end labeling staining (original magnification ×200).

Biotechnology) for 48 hours. Cell proliferation assay was determined by 3-(4, 5-dimethylthiazol-2-yl)-2,5-diphenyl-tetrazolium bromide assay (Sigma, St Louis, MO) described previously.[37] Absorbance at 540 nm was read on a microplate reader (Molecular Devices). All assays were performed in triplicate.

Chemotactic migration assay. The effects of the chimeric proteins on the chemotactic motility of HUVECs responding to $VEGF_{165}$ was assessed using transwell migration chambers (Corning Costar, Cambridge, MA) with 6.5-mm diameter polycarbonate filters (8-μm pore size). Cells in M199 medium containing 1% FBS were stimulated with 0.3 nmol/l $VEGF_{165}$ and

Table 2 Combination treatment with FP3 and 5-fluorouracil (5-FU)

		FTV relative to untreated controls[a]				
				Combination treatment		Ratio of expected FTV/observed FTV[d]
Treatment	Day[b]	FP3	5-FU	Expected[c]	Observed	
FP3+5-FU	21	0.424	0.431	0.183	0.209	0.876
	28	0.204	0.303	0.062	0.161	0.383
	35	0.196	0.439	0.086	0.109	0.788
	42	0.218	0.504	0.11	0.079	1.393

[a]FTV, fractional tumor volume, calculated as mean tumor volume experimental/mean tumor volume control. [b]Day after tumor treatment. [c]Mean FTV of FP3 × mean FTV of 5-FU. [d]Obtained by dividing the expected FTV by the observed FTV. A ratio >1 indicates a synergistic effect, and a ratio <1 indicates a less than additive effect.

treated with 3.5–70 nmol/l bevacizumab, FP1, or FP3 for 30 minutes at room temperature, and then seeded into the lower wells. HUVECs incubated for 4 hours in M199 medium containing 1% FBS were harvested by trypsinization and loaded into the upper wells (1×10^5 cells/well). The chamber was then incubated at 37 °C for 4 hours. Chemotaxis was quantified by counting the migrated cells with an optical microscope (Olympus IX71; Olympus, Melville, NY) in 10 random fields.

Endothelial cell tube formation assay. The formation of HUVEC capillary-like structures on a basement membrane matrix was used to assess the antiangiogenic activity of FP3. The 16 mm-diameter tissue culture plates were coated with 250-µl growth factor-reduced Matrigel (Collaborative Biomedical Products, Bedford, MA) for 30 minutes at 37 °C. HUVECs were seeded on the Matrigel bed (1.5×10^5 cells/well) and cultured in M199 medium containing 350 nmol/l bevacizumab, FP1, or FP3 in the presence of $VEGF_{165}$ (0.3 nmol/l) for 20 hours. M199 medium containing $VEGF_{165}$ alone served as the control. Capillary networks were photographed, and the area covered by the tube network was quantified by Image-Pro Plus software (Media Cybernetics, Silver Spring, MD).

Aortic ring sprouting assay. Aortic ring segments (1 mm) prepared from 6-week-old male Sprague Dawley rats were placed in Matrigel-coated 48-well tissue culture plates, as described previously.[19] The aortic ring segments were incubated in serum-free EBM-2 medium (Cambrex Bio Science Walkersville, Walkersville, MD), and $VEGF_{165}$ (1.2 nmol/l) was added to the wells along with bevacizumab (700 or 1,400 nmol/l) or FP3 (700 or 1,400 nmol/l). Controls were incubated in EBM-2 medium containing $VEGF_{165}$ alone. Visual counts of microvessel outgrowths from explanted cultures ($n = 6$) were performed under bright field microscopy. Results were graded from 0 (no vessel sprouts) to 5 (profuse vessel sprouting).

Western blot analysis. HUVECs were pretreated with bevacizumab, FP1, or FP3 (3 nmol/l) for 30 minutes, followed by treatment with VEGF (0.3 nmol/l) for an additional 10 minutes. Immunoblotting was performed as described previously.[38] Blocked membranes were probed with primary antibodies against AKT, phosphorylated AKT, ERK1/2, and phosphorylated ERK1/2 (1:000 dilution; Cell Signaling Technology, Beverly, MA) overnight at 4 °C. Secondary antibodies conjugated to horseradish peroxidase were visualized by enhanced chemiluminescence substrate (Amersham Pharmacia Biotech AB, Uppsala, Sweden).

Antitumor effects in human tumor xenograft models. HepG2 (1×10^7 cells/mouse) or Lovo (5×10^6 cells/mouse) cells were injected subcutaneously into the right flank of female athymic nude mice that were 5–6 weeks old. For HepG2 tumors, the mice were treated on day 2 after tumor cell implantation by i.v. injection of 200 µl PBS, FP3 (4, 10, or 25 mg/kg), or bevacizumab (10 mg/kg) twice weekly for the indicated time. Similarly, for Lovo tumors, the mice were treated on day 2 following tumor cell implantations by i.v. injection of 200 µl PBS, FP1 (10 mg/kg), or FP3 (10 mg/kg) twice weekly for 7 weeks. MCF-7 cells were injected subcutaneously in the abdomen of nude mice (1×10^7 cells/mouse). When tumors reached an average size of 80–100 mm^3, mice received i.v. injections of FP3 (2, 6, or 18 mg/kg) or bevacizumab (6 mg/kg) twice weekly for 5 weeks. Tumor volumes were determined weekly with calipers (tumor volume = (length × $width^2$)/2) as described previously.[39] Inhibition was determined by the relative tumor growth ratio T/C = TRTV/CRTV × 100%, where TRTV is the relative tumor volume of the treated groups and CRTV is the relative tumor volume of the control group.

Antitumor effects of combination of FP3 with chemotherapeutics. LoVo cells were injected subcutaneously into the right flank of female athymic nude mice (1×10^7 cells/mouse) that were 5–6 weeks old. When the tumors reached an average size of 80 to 100 mm^3, the animals received i.v. injections of PBS, 5-FU (10 mg/kg), FP3 (6 mg/kg), or combination treatment of FP3 and 5-FU. 5-FU was administered once a week and FP3 was administered twice weekly for 7 weeks. The observed data were compared with the predicted maximum and minimum data for the presence of synergism by a statistical analysis using the Stat View 4.01 software program (Abacus Concepts, Berkeley, California) as described previously.[40]

Immunohistochemistry. LoVo xenograft tumors were fixed in formalin-free IHC zinc fixative (BD Biosciences Pharmingen, San Diego, CA), embedded in paraffin, and sectioned at 5 µm. Staining for mouse vessels was performed by incubating sections with a monoclonal antibody against mouse CD31 specific for endothelial cells (BD Biosciences Pharmingen) at 4°C overnight. Sections were then incubated with a biotinylated polyclonal anti-rat antibody (BD Biosciences Pharmingen), followed by avidin coupled to biotinylated horseradish peroxidase. Sections were then developed with DAB (Dako, Carpinteria, CA) and counterstained with Meyer's hematoxylin. Microvessel density was quantitated by ProImage software. Tumor tissue sections (5-µm) fixed in 4% formaldehyde were stained for apoptotic cells using an *in situ* cell death detection kit (Boehringer Mannheim, Ridgefield, CT), as previously described.[39]

Statistical analysis. Data are presented as mean ± SE of the mean (SEM) and analyzed by SPSS 16.0 software (SPSS, Chicago, IL). Group results were compared by one-way analysis of variance. $P < 0.05$ was considered significant.

SUPPLEMENTARY MATERIAL

Figure S1. Effects of FP3 on $VEGF_{165}$-induced human umbilical vein endothelial cell (HUVEC).

ACKNOWLEDGMENTS

This work was supported by grants from the Ministry of Knowledge Economy (10030051, Dr C.-O.Yun), the Korea Food and Drug Administration (KFDA-10172-332 to Dr C.-O.Yun), and the National Research Foundation of Korea (R15-2004-024-02001-0, 2010-0029220, 2009K001644, Dr C.-O.Yun). Jung-Sun Lee, Ji Young Yoo, and Hyewon Shin are graduate students sponsored by the Brain Korea 21 Project for Medical Science, Yonsei University College of Medicine, Seoul, South Korea.

REFERENCES

1. Hanahan, D and Folkman, J (1996). Patterns and emerging mechanisms of the angiogenic switch during tumorigenesis. *Cell* **86**: 353–364.
2. Ferrara, N and Alitalo, K (1999). Clinical applications of angiogenic growth factors and their inhibitors. *Nat Med* **5**: 1359–1364.
3. Holash, J, Davis, S, Papadopoulos, N, Croll, SD, Ho, L, Russell, M *et al.* (2002). VEGF-Trap: a VEGF blocker with potent antitumor effects. *Proc Natl Acad Sci* USA **99**: 11393–11398.
4. Kim, KJ, Li, B, Winer, J, Armanini, M, Gillett, N, Phillips, HS *et al.* (1993). Inhibition of vascular endothelial growth factor-induced angiogenesis suppresses tumour growth in vivo. *Nature* **362**: 841–844.
5. Yancopoulos, GD, Davis, S, Gale, NW, Rudge, JS, Wiegand, SJ and Holash, J (2000). Vascular-specific growth factors and blood vessel formation. *Nature* **407**: 242–248.
6. Keyt, BA, Nguyen, HV, Berleau, LT, Duarte, CM, Park, J, Chen, H *et al.* (1996). Identification of vascular endothelial growth factor determinants for binding KDR and FLT-1 receptors. Generation of receptor-selective VEGF variants by site-directed mutagenesis. *J Biol Chem* **271**: 5638–5646.
7. Shalaby, F, Rossant, J, Yamaguchi, TP, Gertsenstein, M, Wu, XF, Breitman, ML *et al.* (1995). Failure of blood-island formation and vasculogenesis in Flk-1-deficient mice. *Nature* **376**: 62–66.
8. Fong, GH, Rossant, J, Gertsenstein, M and Breitman, ML (1995). Role of the Flt-1 receptor tyrosine kinase in regulating the assembly of vascular endothelium. *Nature* **376**: 66–70.
9. Volm, M, Koomägi, R and Mattern, J (1997). Prognostic value of vascular endothelial growth factor and its receptor Flt-1 in squamous cell lung cancer. *Int J Cancer* **74**: 64–68.
10. Lu, D, Kussie, P, Pytowski, B, Persaud, K, Bohlen, P, Witte, L *et al.* (2000). Identification of the residues in the extracellular region of KDR important for interaction with vascular endothelial growth factor and neutralizing anti-KDR antibodies. *J Biol Chem* **275**: 14321–14330.
11. Asano, M, Yukita, A, Matsumoto, T, Hanatani, M and Suzuki, H (1998). An anti-human VEGF monoclonal antibody, MV833, that exhibits potent anti-tumor activity in vivo. *Hybridoma* **17**: 185–190.
12. Kamiya, K, Konno, H, Tanaka, T, Baba, M, Matsumoto, K, Sakaguchi, T *et al.* (1999). Antitumor effect on human gastric cancer and induction of apoptosis by vascular endothelial growth factor neutralizing antibody. *Jpn J Cancer Res* **90**: 794–800.
13. Prewett, M, Huber, J, Li, Y, Santiago, A, O'Connor, W, King, K *et al.* (1999). Antivascular endothelial growth factor receptor (fetal liver kinase 1) monoclonal antibody inhibits tumor angiogenesis and growth of several mouse and human tumors. *Cancer Res* **59**: 5209–5218.
14. Ferrara, N, Chen, H, Davis-Smyth, T, Gerber, HP, Nguyen, TN, Peers, D *et al.* (1998). Vascular endothelial growth factor is essential for corpus luteum angiogenesis. *Nat Med* **4**: 336–340.
15. Gerber, HP, Vu, TH, Ryan, AM, Kowalski, J, Werb, Z and Ferrara, N (1999). VEGF couples hypertrophic cartilage remodeling, ossification and angiogenesis during endochondral bone formation. *Nat Med* **5**: 623–628.
16. Martin, L and Schilder, R (2007). Novel approaches in advancing the treatment of epithelial ovarian cancer: the role of angiogenesis inhibition. *J Clin Oncol* **25**: 2894–2901.
17. Kamba, T and McDonald, DM (2007). Mechanisms of adverse effects of anti-VEGF therapy for cancer. *Br J Cancer* **96**: 1788–1795.
18. O'Reilly, MS (2002). The combination of antiangiogenic therapy with other modalities. *Cancer J* **8 Suppl 1**: S89–S99.
19. Jain, RK, Duda, DG, Clark, JW and Loeffler, JS (2006). Lessons from phase III clinical trials on anti-VEGF therapy for cancer. *Nat Clin Pract Oncol* **3**: 24–40.
20. Shinkai, A, Ito, M, Anazawa, H, Yamaguchi, S, Shitara, K and Shibuya, M (1998). Mapping of the sites involved in ligand association and dissociation at the extracellular domain of the kinase insert domain-containing receptor for vascular endothelial growth factor. *J Biol Chem* **273**: 31283–31288.
21. Fuh, G, Li, B, Crowley, C, Cunningham, B and Wells, JA (1998). Requirements for binding and signaling of the kinase domain receptor for vascular endothelial growth factor. *J Biol Chem* **273**: 11197–11204.
22. Kuhn, H, Hammerschmidt, S and Wirtz, H (2007). Targeting tumorangiogenesis in lung cancer by suppression of VEGF and its receptor - results from clinical trials and novel experimental approaches. *Curr Med Chem* **14**: 3157–3165.
23. Ferrara, N (1995). The role of vascular endothelial growth factor in pathological angiogenesis. *Breast Cancer Res Treat* **36**: 127–137.
24. Zhu, Z and Witte, L (1999). Inhibition of tumor growth and metastasis by targeting tumor-associated angiogenesis with antagonists to the receptors of vascular endothelial growth factor. *Invest New Drugs* **17**: 195–212.
25. Millauer, B, Shawver, LK, Plate, KH, Risau, W and Ullrich, A (1994). Glioblastoma growth inhibited *in vivo* by a dominant-negative Flk-1 mutant. *Nature* **367**: 576–579.
26. Skobe, M, Rockwell, P, Goldstein, N, Vosseler, S and Fusenig, NE (1997). Halting angiogenesis suppresses carcinoma cell invasion. *Nat Med* **3**: 1222–1227.
27. Gerber, HP, McMurtrey, A, Kowalski, J, Yan, M, Keyt, BA, Dixit, V *et al.* (1998). Vascular endothelial growth factor regulates endothelial cell survival through the phosphatidylinositol 3'-kinase/Akt signal transduction pathway. Requirement for Flk-1/KDR activation. *J Biol Chem* **273**: 30336–30343.
28. Gupta, K, Kshirsagar, S, Li, W, Gui, L, Ramakrishnan, S, Gupta, P *et al.* (1999). VEGF prevents apoptosis of human microvascular endothelial cells via opposing effects on MAPK/ERK and SAPK/JNK signaling. *Exp Cell Res* **247**: 495–504.
29. Ross, J (1996). Comments on the article "Persistent confusion of total entropy and chemical system entropy in chemical thermodynamics" [(1996) Proc. Natl. Acad. Sci. USA 93, 7452-7453]. *Proc Natl Acad Sci USA* **93**: 14314; discussion 14315.
30. Holmgren, L, O'Reilly, MS and Folkman, J (1995). Dormancy of micrometastases: balanced proliferation and apoptosis in the presence of angiogenesis suppression. *Nat Med* **1**: 149–153.
31. Mauceri, HJ, Hanna, NN, Beckett, MA, Gorski, DH, Staba, MJ, Stellato, KA *et al.* (1998). Combined effects of angiostatin and ionizing radiation in antitumour therapy. *Nature* **394**: 287–291.
32. Teicher, BA, Williams, JI, Takeuchi, H, Ara, G, Herbst, RS and Buxton, D (1998). Potential of the aminosterol, squalamine in combination therapy in the rat 13,762 mammary carcinoma and the murine Lewis lung carcinoma. *Anticancer Res* **18**(4A): 2567–2573.
33. Katoh, O, Tauchi, H, Kawaishi, K, Kimura, A and Satow, Y (1995). Expression of the vascular endothelial growth factor (VEGF) receptor gene, KDR, in hematopoietic cells and inhibitory effect of VEGF on apoptotic cell death caused by ionizing radiation. *Cancer Res* **55**: 5687–5692.
34. Katoh, O, Takahashi, T, Oguri, T, Kuramoto, K, Mihara, K, Kobayashi, M *et al.* (1998). Vascular endothelial growth factor inhibits apoptotic death in hematopoietic cells after exposure to chemotherapeutic drugs by inducing MCL1 acting as an antiapoptotic factor. *Cancer Res* **58**: 5565–5569.
35. Zhang, M, Zhang, J, Yan, M, Luo, D, Zhu, W, Kaiser, PK *et al.* (2011). A phase 1 study of KH902, a vascular endothelial growth factor receptor decoy, for exudative age-related macular degeneration. *Ophthalmology* **118**: 672–678.
36. Zhang, M, Zhang, J, Yan, M, Li, H, Yang, C and Yu, D (2008). Recombinant anti-vascular endothelial growth factor fusion protein efficiently suppresses choridal neovasularization in monkeys. *Mol Vis* **14**: 37–49.
37. Yoo, JY, Kim, JH, Kim, J, Huang, JH, Zhang, SN, Kang, YA *et al.* (2008). Short hairpin RNA-expressing oncolytic adenovirus-mediated inhibition of IL-8: effects on antiangiogenesis and tumor growth inhibition. *Gene Ther* **15**: 635–651.
38. Lee, JS, Song, SH, Kim, JM, Shin, IS, Kim, KL, Suh, YL *et al.* (2008). Angiopoietin-1 prevents hypertension and target organ damage through its interaction with endothelial Tie2 receptor. *Cardiovasc Res* **78**: 572–580.
39. Kwon, OJ, Kim, PH, Huyn, S, Wu, L, Kim, M and Yun, CO (2010). A hypoxia- and {alpha}-fetoprotein-dependent oncolytic adenovirus exhibits specific killing of hepatocellular carcinomas. *Clin Cancer Res* **16**: 6071–6082.
40. Yu, DC, Chen, Y, Dilley, J, Li, Y, Embry, M, Zhang, H *et al.* (2001). Antitumor synergy of CV787, a prostate cancer-specific adenovirus, and paclitaxel and docetaxel. *Cancer Res* **61**: 517–525.